International Journal of Engineering

Journal Homepage: www.ije.ir

# Fabrication and Evaluation of Controlled Release of Doxorubicin Loaded UiO-66-$NH_2$ Metal Organic Frameworks

N. Rakhshani[a], N. Hassanzadeh Nemati*[a], A. Ramazani Saadatabadi[b], S. K. Sadrnezhaad[c]

[a] *Department of Biomedical Engineering, Science and Research Branch, Islamic Azad University, Tehran, Iran*
[b] *Department of Chemical and Petroleum Engineering, Sharif University of Technology, Tehran, Iran*
[c] *Department of Materials Science and Engineering, Sharif University of Technology, Tehran, Iran*

*PAPER INFO*

*Paper history:*
Received 18 March 2021
Received in revised form 18 May 2021
Accepted 12 June 2021

*Keywords*:
*Metal Organic Framework*
*UiO-66-$NH_2$*
*Doxorubicin*
*Controlled Release*
*Biocompatibility*

*ABSTRACT*

The metal-organic frameworks (MOFs) due to their large specific surface area and high biocompatibility are suitable as carriers for drug delivery systems (DDSs). In the present study, doxorubicin (DOX) as an anticancer drug was loaded into UiO-66-$NH_2$ MOFs to decrease the adverse side effects of pristine DOX use and to increase its efficiency through the controlled release of DOX from MOFs. The MOFs were synthesized via microwave heating method and characterized using X-ray diffraction, scanning electron microscopy, and Brunauer-Emmett- Teller analysis. The drug loading efficiency, drug release profiles from synthesized MOFs and pharmacokinetic studies were investigated. The biocompatibility of drug-loaded-UiO-66-$NH_2$ MOFs was also evaluated by their incubation in L929 normal fibroblast cells. The average particle sizes of UiO-66-$NH_2$ MOFs and DOX loaded-MOFs were found to be 175 nm, and 200 nm respectively. The Brunauer-Emmett- Teller surface area of UiO-66-NH2 MOFs and DOX (100 μg $mL^{-1}$) loaded-UiO-66-$NH_2$ MOFs were estimated to be 1052 $m^2g^{-1}$, and 121 $m^2g^{-1}$, respectively. The synthesized MOFs exhibited high capability for the controlled release of DOX from MOFs as a pH sensitive carrier. The DOX release data were best described using Korsmeyer-Peppas pharmacokinetic model ($R2 \geq 0.985$). The cell viability of synthesized MOFs against fibroblast normal cells was found to be higher than 90%. It could be concluded that the UiO-66-$NH_2$ MOFs could be used as an effective pH sensitive carrier for loading anticancer drugs.

***doi**: 10.5829/ije.2021.34.08b.08*

## 1.INTRODUCTION

The main challenges of traditional drug delivery systems are their poor controlled release and low dosage of anticancer agents in targeted tissue [1]. Furthermore, the use of pristine anticancer drugs due to their high toxicity and adverse effect on normal tissues is limited [2]. For example, although doxorubicin (DOX) as an anticancer agent has been applied for the various cancers treatment such as lung, brain, prostate, breast, and skin; its use is associated with many limitations such as toxic side effects and the low therapeutic efficiency due to its low half time of 1.8 h [3]. To reduce the adverse effects of DOX to patients and to increase the chemotherapy efficacy, various drug delivery systems such as hydrogels [3], liposomes [4], micelles [5], nanofibers [6], and inorganic materials [7] have been developed for controlled release of DOX. Among inorganic materials used in biomedical applications such as carbon based-materials [8], metal oxides [9], zeolites [7], silver [10], and metal-organic frameworks (MOFs) [11-14], MOFs as a new class of crystalline porous materials due to their higher specific surface area, and large porosity in compare to other inorganic materials have been developed for biomedical applications. The nanosized-MOFs (NMOFs) exhibited unique physicochemical properties such as the higher specific surface area in compare to the micrometer scale of MOFs which provide the high loading of drugs and high chemotherapeutic efficacy [14, 15]. Various NMOFs such as ZIF-8 [16], MIL 101 [17] and UiO-66 [18, 19] have been used for drug delivery systems. UiO-66 consisted of $[Zr_6O_4(OH)_4]$

*Corresponding Author Institutional Email: hasanzadeh@srbiau.ac.ir (N. Hassanzadeh Nemati)

Please cite this article as: N. Rakhshani, N. Hassanzadeh Nemati, A. Ramazani Saadatabad[b], S. K. Sadrnezhaad, Fabrication and Evaluation of Controlled Release of Doxorubicin Loaded UiO-66-$NH_2$ Metal Organic Frameworks, International Journal of Engineering, Transactions B: Applications, Vol. 34, No. 08, (2021) 1874-1881

octahedral (11 Å) and tetrahedral (8 Å) cages in 1:2 ratio and 1,4-benzenedicarboxyle acid ($H_2$bdc) ligands is synthesized by various methods such as hydrothermal, solvothermal, microwave and microreactor technology [20]. The heterogeneous reaction takes place under high pressure and high temperature conditions in the hydro/solvothermal methods which could be resulted in generation of large crystals with microsized particles [21]. The ultrasonic method provides the changes in the physicochemical properties of molecules under ultrasonic irradiation ranging from 20 kHz–10 MHz. However, the rate of sonochemical reduction completely depends on the ultrasonic frequency and thus, the heat-sensitive materials cannot withstand the acoustic cavitation at higher ultrasonic frequency [22, 23]. The microwave heating method has advantages over other synthetic methods such as the use of lower temperature, shorter reaction time, control of morphology and phase as well as the synthesis of finer particles with higher specific surface area [24]. Furthermore, the uniform absorption of energy throughout the entire volume of MOFs compared to conventional oven heating methods leads to homogeneous nucleation and reduction in crystallization time followed by production of the microporous MOFs for loading of the high content of drug [25]. Whereas, the longer time of conventional methods for MOFs synthesis leads to the production of microsized-MOF particles with lower high specific surface area [26].

UiO-66 as a zirconium-based MOF has unique properties such as high mechanical properties and water stability which facilitate its use for environmental and biomedical applications [27-29]. UiO-66 MOFs due to having high stability in aqueous solutions and bloodstream as well as high biocompatibility could be considered as an ideal candidate for drug delivery of anticancer drugs such as DOX, paclitaxel, etc. [29, 30]. Moreover, the presence of open cavities in the UiO-66 MOF matrix led to incorporate the high content of drug molecules. Furthermore, UiO-66 MOF could be considered as a pH-sensitive carrier for the controlled release of anticancer agents into the cancer tissues [29]. The delivery of calcein as a hydrophilic drug into the UiO-66 MOF was studied by the Orellana-Tavra et al. [30]. Nasrabadi et al. [19] synthesized the UiO-66 metal-organic framework nanoparticles via a solvothermal method for the controlled release of ciprofloxacin. In the present study, DOX anticancer drug was loaded into UiO-66-$NH_2$ MOFs synthesized by the microwave heating method. The synthesized UiO-66-$NH_2$ MOFs and DOX loaded-UiO-66-$NH_2$ MOFs were characterized using XRD, SEM, and BET analysis. The drug loading efficiency, drug release, and kinetic studies were investigated.

## 2. MATERIALS AND METHODS

**2. 1. Materials** 2-Aminoterephthalic acid (BDC-$NH_2$, purity ≥ 99.9%), and zirconium chloride ($ZrCl_4$, purity ≥ 99.9%) were supplied from Sigma–Aldrich (Germany). N,N Dimethylformamide (DMF, purity≥99.0%), and hydrochloric acid (HCl, 37%) were purchased from Fluka (Switzerland). Doxorubicin was provided by Sobhan Darou Co. (Iran).

**2. 2. Synthesis of UiO-66-$NH_2$** The UiO-66-$NH_2$ MOF particles were synthesized by microwave method as described previously by Jamshidifard et al. [31]. Briefly, 125 mg $ZrCl_4$, 134 mg BDC-$NH_2$, 15 mL DMF and 1 mL HCl were mixed under sonication for 1 h. Then, the mixture was poured into the glass bottle. The microwave heating was proceeded into a microwave oven (CE1110 C, Samsung, Korea) with 900 W power and wavelength of 2.45 GHz at 130°C for 1 h. The temperature of the glass bottle was measured by a Teflon-coated thermocouple (TC4Y, Autonics, Korea). Then, the product was washed with DMF and methanol three times and dried at 60 °C for 6 h [32].

**2. 3. Loading of DOX into the UiO-66-$NH_2$** To load DOX molecules into the UiO-66-$NH_2$ MOFs, 5 mg UiO-66-$NH_2$ NMOFs were dispersed into 10 mL DOX solutions (10, 50, and 100 μg $mL^{-1}$) for 24 h under stirring. Then, the prepared UiO-66-$NH_2$/DOX NMOFs were washed with ethanol and distilled water three times. Then, the prepared products were centrifuged at 12000 rpm for 20 min. The final DOX loading efficiency (%) in NMOFs samples was determined after centrifugation of NMOFs using UV-Vis spectrophotometer at the wavelength of 481 nm as follow:

$$DEE\,(\%) = \frac{Final\ \ content\ \ of\ \ drugs\ \ in\ \ samples}{Initial\ \ content\ \ of\ \ drugs\ \ doped - samples} \times 100 \qquad (1)$$

**2. 4. Characterization Tests** To confirm the structure and crystallinity of NMOFs, the X-ray diffraction (XRD) patterns of MOF samples were recorded at 25 °C using Philips X'pert diffractometer ranging from 10–80° with Cu-Kα radiation. The functional groups of DOX, UiO-66-$NH_2$, and UiO-66-$NH_2$/DOX were determined using Fourier-transform infrared spectroscopy (FTIR) on an Equinox 55 FTIR spectrometer ranging from 4000-400 $cm^{-1}$. The morphology of NMOFs was investigated using scanning electron microscopy (TESCAN, VEGA 3SB) and field emission scanning electron microscopy (FESEM, MIRA3TESCAN-XMU). The specific surface area of NMOFs was determined using Brunauer-Emmett- Teller (BET) method. The concentration of DOX was

determined using UV-Vis spectrophotometer (JAS.CO V-530, Japan) at wavelength of 481 nm. The hydrodynamic diameter and size distribution of the UiO-66-$NH_2$ MOFs and DOX loaded-MOFs were determined using dynamic light scattering (DLS) by a Malvern Zetasizer Nano (Malvern Instruments, Worcestershire).

**2. 5. Drug Release and Kinetic Studies** To achieve the DOX release from synthesized MOFs, 50 mg drug-loaded-MOFs were incubated at 37 °C in 2 mL Phosphate-buffered saline (PBS) and then sealed into a dialysis bag (molecular cut off 50 kD). Then, the samples were soaked in 20 mL of 0.1M PBS (pH values of 7.4 and 5.5). The suspensions were transferred into a thermostated shaking water bath (Hidolff) at 37 °C and 100 rpm for 3 days. At certain times (0.5 h, 1 h, 2h, 3h, 6h, 9 h, 12 h, 24h, 30 h, 36 h, 42 h, 48 h, 60 h and, 72 h), 2.0 mL of released solution was taken from the dissolution medium, while 2 mL of fresh buffer solution was added to the incubation medium. The final content of DOX was determined using UV-Vis spectroscopy. The DOX release percentage was calculated based on the actual drug content in the UiO-66-$NH_2$ MOFs.The DOX release data were analyzed using zero-order, Higuchi and Korsmeyer-Peppas pharmacokinetic models [6]. The experiments were repeated five times and the average values were reported.

**2. 6. Cell Viability** To investigate the biocompatibility of MOFs samples, the synthesized nanoparticles were incubated in the L929 normal fibroblast cells (Institute Pasteur of Iran, IPI, Tehran, Iran) cultured in RPMI with 10% fetal calf serum and 1% penicillin-streptomycin at 37°C in a humidified atmosphere of 5% $CO_2$. The experiments were repeated three times and the average values were reported.

**2. 7. Statistical Analysis** The statistical analysis was performed by one-way analysis of variance using SPSS version 18 to define the statistically significant values as $P < 0.05$.

## 3. RESULTS AND DISCUSSION

**3. 1. Characterization of UiO-66-$NH_2$ and DOX Loaded- UiO-66-$NH_2$** The XRD patterns of DOX, UiO-66-$NH_2$, and DOX loaded- UiO-66-$NH_2$ NMOFs are illustrated in Figure 1. The presence of sharp diffraction peaks at $2\theta=7.5^{\circ}$ and $8.5^{\circ}$ corresponding to (111), and (002) planes indicated the formation of pure UiO-66-$NH_2$ MOF nanoparticles [31]. It can be seen that there are sharp peaks in the XRD pattern of DOX, which demonstrated the crystalline form of pristine DOX. Incorporation of DOX into the MOF resulted in the weakening of diffraction peaks of UiO-66-$NH_2$ MOF due to decreasing the X-ray contrast of MOF pore cages. Furthermore, no diffraction peaks were detected in the XRD pattern of UiO-66/DOX MOF nanoparticles, which indicated the amorphous status of DOX after loading DOX into the UiO-66-$NH_2$ MOF particles in comparison with the crystalline form of pristine DOX, which is consistent with the pores' size being small scale not supporting aggregation into a crystalline form [33]. A similar trend was reported by Farboudi et al. [32] for doxorubicin and folic acid/UiO-66-$NH_2$ loaded-nanofibers.

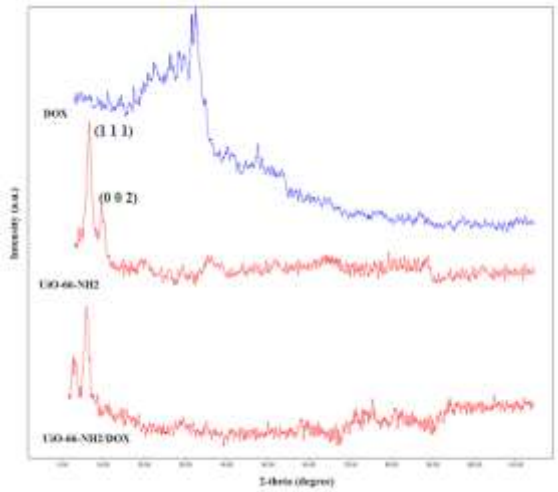


**Figure 1.** XRD patterns of DOX, UiO-66-$NH_2$ and DOX loaded- UiO-66-$NH_2$ NMOFs

The SEM images of UiO-66-$NH_2$ NMOFs and DOX loaded- UiO-66-$NH_2$ NMOFs are illustrated in Figure 2. As shown, the uniform nanoparticles ranging from 100-300 nm were obtained for UiO-66-$NH_2$ MOF particles. The average particle sizes of UiO-66-$NH_2$ NMOFs and DOX loaded- UiO-66-$NH_2$ NMOFs were found to be 175 nm and 200 nm, respectively. The FESEM image of the synthesized UiO-66-$NH_2$ MOF nanoparticles revealed the presence of various shapes including spherical and polyhedral shapes of UiO-66-$NH_2$ MOF (Figure 1C). An increase in the particle sizes of DOX loaded- UiO-66-$NH_2$ NMOFs may be attributed to the aggregation of some UiO-66-$NH_2$ particles during the incorporation of DOX into the UiO-66-$NH_2$ matrix. An increase in particle sizes was further confirmed by the dynamic light scattering (DLS) measurement. As shown, the average hydrodynamic sizes of UiO-66-$NH_2$ NMOFs and DOX loaded- UiO-66-$NH_2$ NMOFs were found to be about 230 nm and 275 nm, respectively. The average particle sizes of synthesized NMOFs reported by SEM were lower than that of DLS. The hydrodynamic radius of MOFs was found to be higher than that of particle size of dried nanoparticles. Similar trends were reported by other researchers [34, 35].

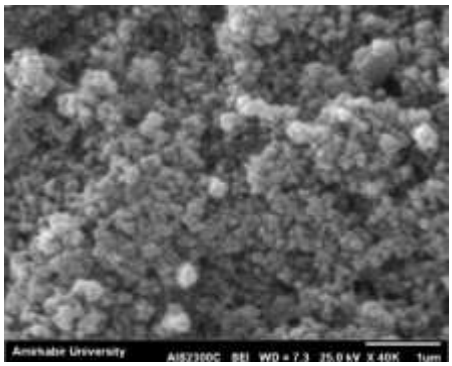


(a)

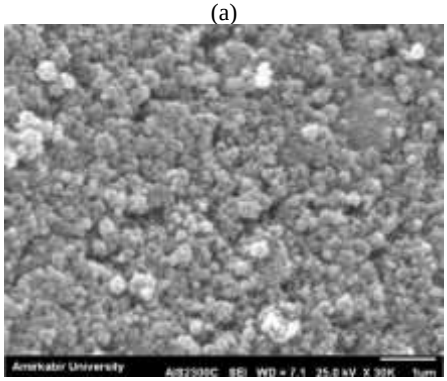


(b)

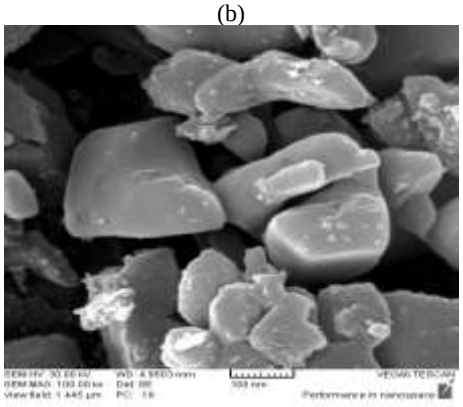

(c)

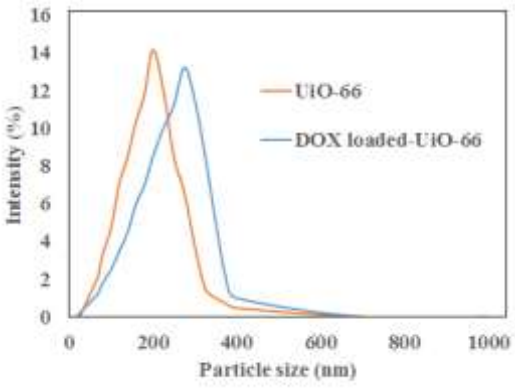


(d)

**Figure 2.** SEM images of (A) UiO-66-$NH_2$ NMOFs, (B) DOX loaded-UiO-66-$NH_2$ NMOFs, (C) FESEM image of UiO-66-$NH_2$ NMOFs, and (D) DLS of synthesized UiO-66-$NH_2$ NMOFs and DOX loaded- UiO-66-$NH_2$

The FTIR spectra of UiO-66-$NH_2$ and DOX loaded-UiO-66-$NH_2$ are illustrated in Figure 3. For UiO-66-$NH_2$ MOFs, the observed peaks at 3450 $cm^{-1}$ and 3360 $cm^{-1}$ were assigned to the stretching vibrations of OH and NH, respectively. The detected peaks at 1575 $cm^{-1}$and 1390 $cm^{-1}$ were due to the carboxylate groups of BDC-$NH_2$. The Zr($\mu_3$) O bands of MOF were detected at wavenumbers of 730 $cm^{-1}$, 665 $cm^{-1}$, and 560 $cm^{-1}$. After loading of DOX into the MOFs, the observed new peaks at 1710 $cm^{-1}$ and 1610 $cm^{-1}$ corresponding to the C=O and C=C groups of DOX demonstrated the successful doping of DOX into the MOFs. A similar trend was reported by Farboudi et al. [32] after loading DOX into the nanofibers. The BET surface area and pore volume of UiO-66-$NH_2$ NMOFs vs. DOX loaded- UiO-66-$NH_2$ NMOFs were found to be 1052 $m^2g^{-1}$ and 0.58 $cm^2g^{-1}$ vs. 121 $m^2g^{-1}$ and 0.12 $cm^2g^{-1}$, respectively. The obtained results demonstrated the high loading of DOX molecules into the MOF particle pores. The blockage of NMOFs pores by the DOX molecules resulted in significant decrease in specific BET surface area after loading of DOX into the NMOFs. Chowdhuri et al. [29] indicated that the surface area of UCNP@ UiO-66-$NH_2$ /FA was decreased from 932 $m^2g^{-1}$ to 186 $m^2g^{-1}$ after loading of DOX into the MOFs.

**3. 2. Drug Encapsulation Efficiency, Drug Release and Kinetic Studies** The DOX encapsulation efficiency for NMOFs incubated at 10 µg $mL^{-1}$, 50 µg $mL^{-1}$ and 100 µg $mL^{-1}$ DOX is presented in Table 1. As shown, the maximum drug encapsulation efficiency (DEE %) was found to be 53.5% from NMOFs containing 10 µg $mL^{-1}$DOX. By increasing DOX concentration, the DEE was gradually decreased. The

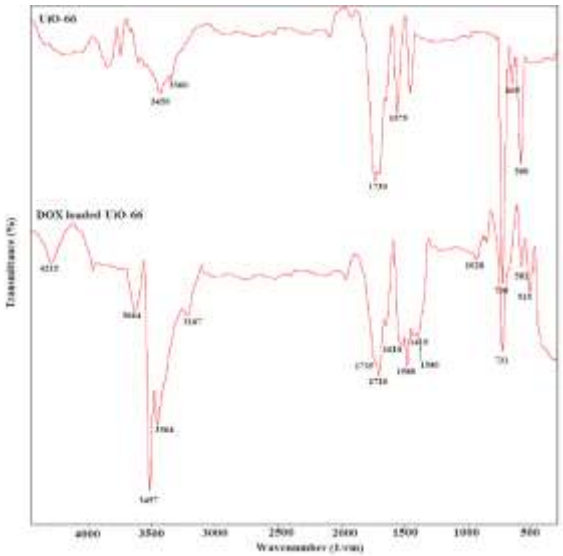


**Figure 3.** FTIR spectra of UiO-66-$NH_2$ and DOX loaded-UiO-66-$NH_2$ NMOFs

**TABLE 1.** Drug encapsulation efficiency of synthesized UiO-66-$NH_2$/DOX (n=5)

| DOX concentration ($\mu g m^{-1}$) | Drug loading efficiency (%) |
|---|---|
| 10 | 53.5±1.5 |
| 50 | 51.3±1.7 |
| 100 | 50.2±1.8 |

higher percentage of drug lost in the loading medium by increasing DOX concentration resulted in a decrease in DEE. A similar trend is reported by Kamba et al. [36] for controlled release of doxorubicin against bone cancer treatment.

The DOX release profiles of NMOFs containing 10 μg $mL^{-1}$, 50 μg $mL^{-1}$ and 100 μg $mL^{-1}$ DOX under pH values of 5.5 and 7.4 are illustrated in Figure 4. As shown, the decrease in pH from physiological pH to acidic pH resulted in faster release of DOX from NMOFs. About 80% DOX release occurred from NMOFs containing 10 μg $mL^{-1}$after 24 h, and 36 h at pH values of 5.5, and 7.4, respectively. After that, the cumulative release of DOX did not significantly change. Therefore, 24 h and 36 h could be considered as equilibrium times of the DOX release from NMOFs at pH values of 5.5, and 7.4, respectively under an initial concentration of 10 μg $mL^{-1}$ DOX. Whereas, the increase in drug content in samples resulted in the gradual increase in the release rate of DOX due to the lower distance of DOX molecules. The loss of some interactions between Zr-O clusters and DOX molecules resulted in the faster release of DOX from NMOFs at pH of 5.5 in comparison to DOX release at pH of 7.4. Nasrabadi et al. [19] reported the higher release percentage of ciprofloxacin from UiO-66 at pH 5 (87%) in comparison with its release from UiO-66 at pH 7.4 after 3 days (80%). Chowdhuri et al. [29] indicated that the DOX release from UCNP@ UiO-66-$NH_2$/FA MOF was increased from 30 and 40% to 65 and 72 % at pH 5.5 in compare to the DOX release at physiological pH after 12 h and 24 h, respectively. Due to the large specific surface area of UiO-66-$NH_2$ MOFs, the majority of DOX molecules have been released from the surface of the MOFs which were adsorbed on the MOF surface during loading of DOX into the UiO-66-$NH_2$ MOFs via electrostatic interaction. The drug release from NMOFs occurred during two stages including the faster release from surface and pores near the surface in the first stage and the second stage was the DOX molecules diffusion from inner pores and cages of NMOFs.

The pharmacokinetic parameters and correlation coefficients of pharmacokinetic models are summarized in Table 2. Based on correlation coefficient values, the DOX release data were best described using Korsemeyer-Peppas model ($R^2 > 0.98$) in compare to zero order ($R^2 > 0.88$) and Higuchi ($R^2 > 0.94$) kinetic

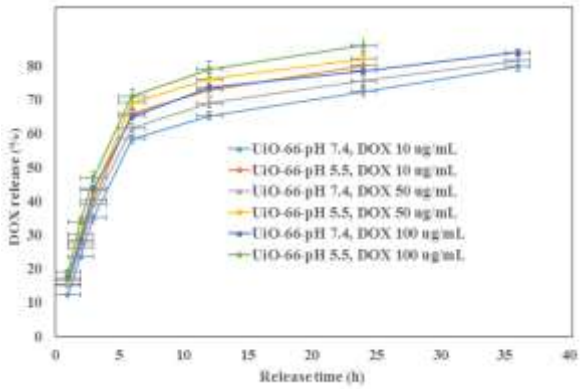


**Figure 4.** DOX release from UiO-66-$NH_2$ NMOFs containing 10, 50 and 100 μg $mL^{-1}$ DOX

**TABLE 2.** Pharmacokinetic parameters of DOX release from UiO-66-$NH_2$ NMOFs

| pH | DOX (μg/mL) | Zero-order | | Higuchi | | Korsmeyer-Peppas | | |
|---|---|---|---|---|---|---|---|---|
| | | $K_0$ ($hr^{-1}$) | $R^2$ | $K_H$ ($hr^{-0.5}$) | $R^2$ | n | $K_{KP}$ | $R^2$ |
| 7.4 | 10 | 0.253 | 0.901 | 3.342 | 0.947 | 0.712 | 4.34 | 0.989 |
| 7.4 | 50 | 0.260 | 0.910 | 3.677 | 0.934 | 0.752 | 4.56 | 0.991 |
| 7.4 | 100 | 0.267 | 0.895 | 4.123 | 0.944 | 0.778 | 5.44 | 0.988 |
| 5.5 | 25 | 0.274 | 0.907 | 4.811 | 0.945 | 0.801 | 5.55 | 0.985 |
| 5.5 | 37 | 0.291 | 0.903 | 4.854 | 0.950 | 0.844 | 5.62 | 0.992 |
| 5.5 | 25 | 0.305 | 0.888 | 4.944 | 0.949 | 0.865 | 5.68 | 0.990 |

models (Table 2). The "n" values of Korsemeyer-Peppas equation indicated the non-Fickian diffusion of the DOX release from MOFs under both pH values of 5.5 and 7.4.

**3. 3. Biocompatibility of NMOFs** The biocompatibility of UiO-66-$NH_2$ and DOX loaded-UiO-66-$NH_2$ was investigated by their incubation in normal fibroblast cells which results are illustrated in Figure 5.

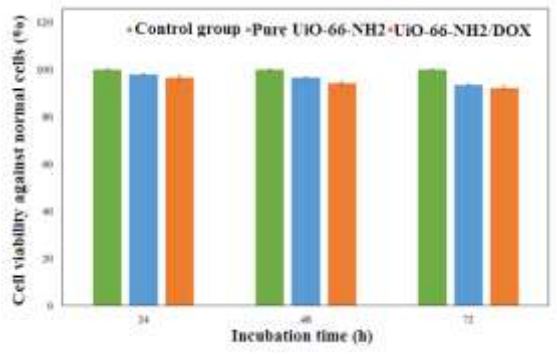


**Figure 5**. Cell viability of UiO-66-$NH_2$, and DOX loaded-UiO-66-$NH_2$ against L929 normal fibroblast cells

The gradual decrease in the cell viability of pure UiO-66-$NH_2$ by time could be attributed to the Zr-O clusters release into the medium which increased the cytotoxicity of fibroblast cells treated with UiO-66-$NH_2$ NMOFs. The cell viability higher than 90% for NMOF samples demonstrated the good biocompatibility of NMOFs for in vivo studies. Orellana-Tavra et al. [30] also indicated that the UiO-66 as a biocompatible and water-stable MOF could be considered as a good candidate for drug delivery applications.

## 4. CONCLUSION

The UiO-66-$NH_2$/DOX NMOFs were successfully synthesized via microwave heating method for controlled release of DOX. The BET surface area and average particle size of UiO-66-$NH_2$ NMOFs and DOX loaded-UiO-66-$NH_2$ NMOFs were found to be 1052 $m^2g^{-1}$, 175 nm and, 121 $m^2g^{-1}$, 200 nm, respectively. The maximum DOX encapsulation efficiency was found to be 53.5% for NMOFs containing 10 μg $mL^{-1}$ DOX. The cumulative release percentage of DOX from NMOF containing 10 μg $mL^{-1}$ was about 80% after 24 h, and 36 h at pH of 5.5, and 7.4, respectively. The non-Fickian diffusion mechanism was achieved by fitting DOX release data with the Korsmeyer-Peppas model. In addition, the high biocompatibility, controlled release manner and high content of DOX in the UiO-66-$NH_2$ NMOFs demonstrated the high capability of the synthesized NMOFs for various cancer treatments.

## 5. REFRENCES


1. Zamboni. W. C, "Liposomal, nanoparticle, and conjugated formulations of anticancer agents", ***Clinical Cancer Research***, Vol.11, No. 23, (2005), 8230-8234, doi: 10.1158/1078-0432.
2. Dizaji. B. F, Khoshbakht. S, Farboudi. A, Azarbaijan. M. H, and Irani. M, "Far-reaching advances in the role of carbon nanotubes in cancer therapy", ***Life Sciences***, Vol. 257, (2020), 118059, doi: 10.1016/j.lfs.2020.118059.
3. Fathi. M, Alami-Milani. M, Geranmayeh. M. H, Barar. J, Erfan-Niya. H, and Omidi. Y, "Dual thermo-and pH-sensitive injectable hydrogels of chitosan/(poly (N-isopropylacrylamide-co-itaconic acid)) for doxorubicin delivery in breast cancer", ***International Journal of Biological Macromolecules***, Vol. 128, (2019), 957-964, doi:10.1016/j.ijbiomac.2019.01.122.
4. Pirouz. F, Najafpour. G, Jahanshahia. M, and Sharifzadeh Baei. M, "Plant-based calcium fructoborate as boron-carrying nanoparticles for neutron cancer therapy", ***International Journal of Engineering, Transactions A: Basics***, Vol. 32, No. 4, (2019), 460-466. doi: 10.5829/ije.2019.32.04a.01.
5. Ma. B, Zhuang. W, Wang. Y, Luo. R, and Wang. Y, pH-sensitive doxorubicin-conjugated prodrug micelles with charge-conversion for cancer therapy. ***Acta Biomaterialia***, Vol. 70, (2018), 186-196, doi: 10.1016/j.actbio.2018.02.008.
6. Abasian. P, Radmansouri. M, Jouybari. M. H, Ghasemi. M. V, Mohammadi. A, Irani. M, and Jazi. F. S, Incorporation of magnetic NaX zeolite/DOX into the PLA/chitosan nanofibers for sustained release of doxorubicin against carcinoma cells death in vitro. ***International Journal of Biological Macromolecules***, Vol. 121, (2019), 398-406, doi: 10.1016/j.ijbiomac.2018.09.215.
7. Rezaei. S, Mohammadi. M, Najafpour. G, D, Moghadamnia. A, Kazemi. S, and Nikzad M, "Separation of curcumin from curcuma longa L. and its conjugation with silica nanoparticles for anti-cancer activities". ***International Journal of Engineering, Transactions B: Applications***, Vol.31, No. 11, (2018), 1803-1809, doi:10.5829/ije.2018.31.11b.01.
8. Bagheri. M, Sangpour. P, Badiei. E, and Pazouki. M, Graphene oxide antibacterial sheets: Synthesis and characterization (research note). ***International Journal of Engineering, Transactions C: Aspects***, Vol. 27, No. 12, (2014), 1803-1808, doi: 10.5829/idosi.ije.2014.27.12c.01
9. Hassanzadeh Nemati. N, and Mirhadi. S. M, "Synthesis and characterization of highly porous $TiO_2$ scaffolds for bone defects", ***International Journal of Engineering, Transactions A: Basics***, Vol. 33, No. 1, (2020), 134-140, doi: 10.5829/ije.2020.33.01a.15.
10. Rozilah. A, Jaafar. C. N, Sapuan, S. M, Zainol. I, and Ilyas. R. A, "The effects of silver nanoparticles compositions on the mechanical, physiochemical, antibacterial, and morphology properties of sugar palm starch biocomposites for antibacterial coating", ***Polymers***, Vol.12, (2020), 2605, doi: 10.3390/polym12112605
11. Huxford. R. C, Della Rocca. J, and Lin. W, "Metal–organic frameworks as potential drug carriers", ***Current Opinion in Chemical Biology,*** Vol. 14, No. 2, (2010), 262-268, doi: 10.1016/j.cbpa.2009.12.012.
12. Zheng. H, Zhang. Y, Liu. L, Wan. W, Guo. P, Nyström. A. M, and Zou. X, "One-pot synthesis of metal–organic frameworks with encapsulated target molecules and their applications for controlled drug delivery", ***Journal of the American Chemical Society***, Vol. 138, No. 3, (2016), 962-968, doi: 10.1021/jacs.5b11720.
13. Beg. S, Rahman. M, Jain. A, Saini. S, Midoux. P, Pichon. C, and Akhter. S, "Nanoporous metal organic frameworks as hybrid polymer–metal composites for drug delivery and biomedical applications". ***Drug Discovery Today***, Vol. 22, No. 4, (2017), 625-637, doi: 10.1016/j.drudis.2016.10.001.
14. Pirzadeh. K, Ghoreyshi. A. A, Rohani. S, and Rahimnejad. M, "Strong Influence of Amine Grafting on MIL-101 (Cr) Metal–Organic Framework with Exceptional $CO_2/N_2$ Selectivity", ***Industrial & Engineering Chemistry Research***, Vol. 59, No. 1, (2019), 366-378, doi: 10.1021/acs.iecr.9b05779.
15. Wang. L, Zheng. M, Xie. Z, "Nanoscale metal–organic frameworks for drug delivery: a conventional platform with new promise", ***Journal of Materials Chemistry B.***, Vol. 6, No. 5, (2018), 707-717, doi: 10.1039/C7TB02970E.
16. Zheng. C, Wang. Y, Phua. S. Z. F, Lim. W. Q, and Zhao. Y, "ZnO–DOX@ ZIF-8 core–shell nanoparticles for pH-responsive drug delivery", ***ACS Biomaterials Science & Engineering***, Vol. 3, No. 10, (2017), 2223-2229, doi: 10.1021/acsbiomaterials.7b00435.
17. Gordon. J, Kazemian. H, and Rohani. S, "MIL-53 (Fe), MIL-101, and SBA-15 porous materials: potential platforms for drug delivery", ***Materials Science and Engineering: C***, Vol. 47, (2015), 172-179, doi: 10.1016/j.msec.2014.11.046.
18. Jarai. B. M, Stillman. Z, Attia. L, Decker. G. E, Bloch. E. D, and Fromen, C. A, "Evaluating UiO-66 metal–organic framework nanoparticles as acid-sensitive carriers for pulmonary drug delivery applications. ***ACS Applied Materials & Interfaces,*** Vol. 12, No. 35, (2020), 38989-39004, doi: 10.1021/acsami.0c10900.
19. Nasrabadi. M, Ghasemzadeh. M. A, and Monfared. M. R. Z, "The preparation and characterization of UiO-66 metal–organic

frameworks for the delivery of the drug ciprofloxacin and an evaluation of their antibacterial activities", ***New Journal of Chemistry***, Vol. 43, No. 40, (2019), 16033-16040, doi: 10.1039/C9NJ03216A.

20. Katz. M. J, Brown. Z. J, Colón. Y. J, Siu. P. W, Scheidt. K. A, Snurr. R. Q, and Farha, O. K. A, "facile synthesis of UiO-66, UiO-67 and their derivatives", ***Chemical Communications***, Vol. 49, No. 82, (2013), 9449-9451, doi:10.1039/C3CC46105J.
21. Gangu. K. K, Maddila. S, Mukkamala. S. B, and Jonnalagadda, S. B. "A review on contemporary metal–organic framework materials", ***Inorganica Chimica Acta***, Vol. 446, (2016) 61-74, doi: 10.1016/j.ica.2016.02.062.
22. Jamkhande. P. G, Ghule. N. W, Bamer. A. H, and Kalaskar, M. G, "Metal nanoparticles synthesis: An overview on methods of preparation, advantages and disadvantages, and applications", ***Journal of Drug Delivery Science and Technology***, Vol. 53, (2019), 101174, doi: 10.1016/j.jddst.2019.101174
23. Rane. A. V, Kanny. K, Abitha. V. K, and Thomas. S, "Methods for synthesis of nanoparticles and fabrication of nanocomposites". In Synthesis of inorganic nanomaterials (pp. 121-139)". (2018). Woodhead Publishing. doi: 10.1016/B978-0-08-101975-7.00005-1.
24. Taddei. M, Dau. P. V, Cohen. S. M, Ranocchiari. M, van Bokhoven. J. A, Costantino. F, and Vivani. R, "Efficient microwave assisted synthesis of metal–organic framework UiO-66: optimization and scale up", ***Dalton Transactions***, Vol. 44, No. 31, (2015), 14019-14026, doi: 10.1039/C5DT01838B.
25. Choi. J. S, Son. W. J, Kim. J, and Ahn. W. S, "Metal–organic framework MOF-5 prepared by microwave heating: Factors to be considered", ***Microporous and Mesoporous Materials***, Vol. 116, No. 1-3, (2008), 727-731, doi: 10.1016/j.micromeso.2008.04.033.
26. Ni. Z, and Masel. R. I, "Rapid production of metal− organic frameworks via microwave-assisted solvothermal synthesis", ***Journal of the American Chemical Society***, Vol. 128, No. 38, (2006), 12394-12395, doi: 10.1021/ja0635231.
27. Pirzadeh. K, Esfandiari. K, Ghoreyshi. A. A, and Rahimnejad, M, "$CO_2$ and $N_2$ adsorption and separation using aminated UiO-66 and $Cu_3$ (BTC) $_2$: A comparative study", ***Korean Journal of Chemical Engineering***, Vol. 37, No.3, (2020), 513-524, doi: 0.1007/s11814-019-0433-5.
28. Pirzadeh. K, Ghoreyshi. A. A, Rahimnejad. M, and Mohammadi. M, "Electrochemical synthesis, characterization and application of a microstructure Cu 3 (BTC) 2 metal organic framework for $CO_2$ and $CH_4$ separation", ***Korean Journal of Chemical Engineering***, Vol. 35, No. 4, (2018), 974-983, doi: 10.1007/s11814-017-0340-6
29. Chowdhuri. A. R, Laha. D, Chandra. S, Karmakar. P, and Sahu. S. K, "Synthesis of multifunctional upconversion NMOFs for targeted antitumor drug delivery and imaging in triple negative breast cancer cells", ***Chemical Engineering Journal***, Vol. 319, (2017), 200-211, doi: 10.1016/j.cej.2017.03.008.
30. Orellana-Tavra. C, Baxter. E. F, Tian. T, Bennett. T. D, Slater. N. K, Cheetham. A. K, and Fairen-Jimenez. D, "Amorphous metal–organic frameworks for drug delivery", ***Chemical Communications***, Vol. 51, No. 73, (2015), 13878-13881, doi: 10.1039/C5CC05237H
31. Jamshidifard. S, Koushkbaghi. S, Hosseini. S, Rezaei. S, Karamipour. A, and Irani. M, "Incorporation of UiO-66-NH2 MOF into the PAN/chitosan nanofibers for adsorption and membrane filtration of Pb (II), Cd (II) and Cr (VI) ions from aqueous solutions", ***Journal of Hazardous Materials***, Vol. 368, (2019), 10-20, doi: 10.1016/j.jhazmat.2019.01.024.
32. Farboudi. A, Mahboobnia. K, Chogan. F, Karimi. M, Askari. A, Banihashem. S, and Irani. M, "UiO-66 metal organic framework nanoparticles loaded carboxymethyl chitosan/poly ethylene oxide/polyurethane core-shell nanofibers for controlled release of doxorubicin and folic acid", ***International Journal of Biological Macromolecules***, Vol. 150, (2020), 178-188, doi: 10.1016/j.ijbiomac.2020.02.067.
33. Suresh. K, and Matzger. A. J, "Enhanced drug delivery by dissolution of amorphous drug encapsulated in a water unstable metal–organic framework (MOF)", ***Angewandte Chemie***, Vol. 131, No. 47, (2019), 16946-16950, doi: 10.1002/ange.201907652.
34. You. J, Li. W, Yu. C, Zhao. C, Jin. L, Zhou. Y, and Wang. O, "Amphiphilically modified chitosan cationic nanoparticles for drug delivery", ***Journal of Nanoparticle Research***, Vol. 15, No. 12, (2013), 1-10, doi: 10.1007/s11051-013-2123-2.
35. Guo. S, Qiao. Y, Wang. W, He. H, Deng. L, Xing. J, and Dong. A, "Poly (ε-caprolactone)-graft-poly (2-(N, N-dimethylamino) ethyl methacrylate) nanoparticles: pH dependent thermo-sensitive multifunctional carriers for gene and drug delivery", ***Journal of Materials Chemistry***, Vol. 20, No. 33 (2010) 6935-6941. DOI: 10.1039/C0JM00506A.
36. Kamba. S. A, Ismail. M, Hussein-Al-Ali. S. H, Ibrahim. T. A. T, and Zakaria. Z. A. B, "In vitro delivery and controlled release of doxorubicin for targeting osteosarcoma bone cancer", **Molecules**, Vol. 18, No. 9, (2013), 10580-10598, doi: 10.3390/molecules180910580.

## Persian Abstract

**چکیده**

چهارچوب‌های آلی–فلزی به علت داشتن سطح ویژه بزرگ و زیست سازگاری بالایشان به عنوان جامل‌های مناسب سیستم‌های رهایش دارو هستند. در این مطالعه، دوکسوروبیسین به عنوان یک داروی ضد سرطان داخل چهارچوب آلی–فلزی $UiO\text{-}66\text{-}NH_2$ سنتز شده به روش مایکروویو بارگذاری شد تا اثرات منفی استفاده از دوکسوروبیسین خالص را کاهش داده و بازده آن از طریق رهایش کنترل شده دارو از چهارچوب آلی فلزی افزایش یابد. سپس چهارچوب آلی فلزی بدون دارو و همچنین با دارو بوسیله آزمون های پراش اشعه ایکس، میکروسکوپ الکترونی روبشی، میکروسکوپ الکترونی روبشی نشر میدانی، طیف سنجی مادون قرمز و اندازه گیری سطح ویژه به روش برنور–ایمیت–تلر مورد ارزیابی قرار گرفت. بازده بارگذاری دارو، پروفایل‌های رهایش دارو و مطالعات فارماکوکینتیکی حاصل از داده‌های رهایش دوکسوروبیسین از نانوذرات چهارچوب آلی–فلزی $UiO\text{-}66\text{-}NH_2$ بررسی شد. زیست سازگاری نانوذرات سنتز شده نسبت به سلول های فیبروبلاست L929 مورد ارزیابی قرار گرفت. اندازه ذرات بدون دارو ۱۷۵ نانومتر و ذرات حاوی دارو ۲۰۰ نانومتر اندازه گیری شد. سطح ویژه برای ذرات بدون دارو ۱۰۵۲ متر مربع بر گرم و برای ذرات حاوی دارو ۱۲۱ مترمربع بر گرم توسط آزمون برنور–ایمیت–تلر اندازه گیری شد. چهارچوب آلی–فلزی سنتز شده توانایی بالایی را برای رهایش کنترل شده دوکسوروبیسین به عنوان یک حامل حساس به pH نشان داد. داده های رهایش دوکسوروبیسین توسط مدل فارکوکینتیکی کورسمیر–پپاس به خوبی تحلیل شد (ضریب همبستگی بیشتر از ۰.۹۸۵). همچنین زیست سازگاری ذرات به وسیله آزمون MTT از طریق غوطه وری آنها در سلول‌های فیبروبلاست بالای ۹۰ درصد حاصل شد. می‌توان نتیجه گرفت که چهارچوب آلی–فلزی $UiO\text{-}66\text{-}NH_2$ می‌تواند به عنوان یک حامل محرک پاسخ حساس به pH برای بارگذاری داروهای ضد سرطان استفاده شود.